

Photon counting techniques with silicon avalanche photodiodes

Henri Dautet, Pierre Deschamps, Bruno Dion, Andrew D. MacGregor,
Darleene MacSween, Robert J. McIntyre, Claude Trottier, and Paul P. Webb

The properties of avalanche photodiodes and associated electronics required for photon counting in the Geiger and the sub-Geiger modes are reviewed. When the Geiger mode is used, there are significant improvements reported in overall photon detection efficiencies (approaching 70% at 633 nm), and a timing jitter (under 200 ps) is achieved with passive quenching at high overvoltages (20–30 V). The results obtained by using an active-mode fast quench circuit capable of switching overvoltages as high as 15 V (giving photon detection efficiencies in the 50% range) with a dead time of less than 50 ns are reported. Larger diodes (up to 1 mm in diameter) that are usable in the Geiger mode and that have quantum efficiencies over 80% in the 500–800-nm range are also reported.

Key words: Photon counting, silicon avalanche photodiode, Geiger-mode operation.

Introduction

Within the past few years, avalanche photodiodes (APD's) have become commercially available, which, when operated in the Geiger mode, have detection efficiencies for single photons in the 20–50% range^{1–4} and dark count rates as low as 10^3 cps at room temperature, which reduce to <10 cps when the APD's are mounted upon a two-stage thermoelectric cooler.⁵ Newer diodes and techniques of using them for which higher detection efficiencies ($\sim 70\%$) and subnanosecond timing jitters have been measured, are now in development. Besides being extremely small and rugged, these devices have rapid recovery from overloads, wide dynamic ranges, very low afterpulsing, relatively low operating voltages (~ 200 – 600 V) compared with photomultiplier tubes, and other properties that make them suitable for use in photon correlation systems.

Structures of Avalanche Photodiodes used in Photon Counting

APD's designed for photon counting are of primarily three types:

(1) Very small (~ 10 - μm diameter), narrow depletion layer (<5 - μm) diodes designed primarily for

doing photon correlation studies with very short (20–50-ps) resolving times. These devices, developed by Cova *et al.* at Politecnico di Milano,⁶ are formed in *p*-type epitaxial layers grown on *n*-type substrates. Early versions of these devices, while achieving very fast responses for light generated within the depletion layer, were plagued by a long tail resulting from carriers absorbed in the substrate and reaching the multiplying region by diffusion. In later versions, the structure was modified to inhibit collection by this mechanism. In the latest version⁷ a FWHM resolution of 50 ps has been achieved while the diffusion tail has been virtually completely suppressed. It should be pointed out that such high speeds, although impressive, are achieved at the price of very small sensitive volumes; such diodes have small areas and maximum quantum efficiencies of $\sim 10\%$ in the 800–900-nm range.

(2) The reach-through APD, commercial versions of which have been available for ~ 20 yr, is a device that is fully depleted and designed to have two distinct field regions: a relatively wide region (30–150 μm , depending on application) of relatively low field ($\sim 20,000$ V/cm) in which light is absorbed and the carriers collected, and a relatively narrow (a few micrometers), high field region in which the multiplication takes place. While these devices were initially designed for use in the linear mode, continual improvements over the years in the reduction of the bulk dark current has permitted smaller versions of these devices (500 μm in diameter, 30 μm thick) to be used in

The authors are with EG&G Optoelectronics, Canada, 22001 Dumberry Road, Vaudreuil, Quebec, Canada, J7V 8P7.

Received 2 October 1992.

the Geiger mode. Much of the published literature on Geiger-mode APD's uses either the EG&G C30902S or the EG&G C30921S version of these devices.

(3) A relatively new superlow- k (or Slik™, EG&G) structure, in which the device has been designed specifically for properties that lead to high single-photon detection efficiencies in the photon counting mode. Small (< 150 μm in diameter) versions of this device have been available for ~ 3 yr; larger versions (up to 1 mm in diameter) are reported in this paper.

The electric-field profile of these devices is sketched in Fig. 1. For the Slik structure, the field profile is designed to achieve the lowest possible value of the effective k value (a weighted ratio of the ionization coefficients of holes to that of electrons⁸) for a given device thickness. This is accomplished by ensuring that the electric field is high enough to give some multiplication everywhere in the device, with the field gradually increasing to reach a maximum near the n^+ contact, where the hole current density is 0. This design results in a breakdown voltage of ~ 400 V and a k_{eff} of ~ 0.002 in a device ~ 25 – 30 μm thick. Lower k_{eff} values at higher breakdown voltages can be achieved with thicker devices.

Theoretically Achievable Photon Detection Efficiency

Photon detection efficiency P_d of an APD can be written as $P_d = \eta P_e$, where η is the quantum efficiency (number of collected primary electron-hole (e-h) pairs per photon incident upon the sensitive area), and P_e is the photoelectron detection efficiency, i.e., the probability that the primary photogenerated e-h pair initiates a pulse of adequate gain to be counted. These two quantities are essentially independent; both must be optimized in order to achieve a good overall detection efficiency.

Quantum Efficiency

With the proper antireflection coating on both the diode and on the window, the quantum efficiency of an APD can be in the 70–95% range in any desired part of the visible spectrum from ~ 500 to 850 nm. Below ~ 500 nm, η is dependent on the thickness of the diffused surface layer, and special processing is required for assuring high quantum efficiency. At 400 nm, for example, the absorption coefficient of silicon is $\sim 10^5/\text{cm}$, so most of the light is absorbed within 0.1 μm of the surface; many of the generated e-h pairs will recombine at the surface unless the doping profile creates a built-in electric field that collects them quickly. Above 850 nm the absorption coefficient is low enough so that some light penetrates the active portion of the depletion layer without being absorbed. For EG&G diodes designed for photon counting, this active region thickness is ~ 25 to 35 μm .

Photoelectron Detection Probability

This depends on the mode of operation. APD's can be operated in three different modes: linear (or proportional), sub-Geiger, and Geiger (in these two last cases, the output is nonproportional to the input).

Geiger-mode operation: The most commonly used mode is the Geiger mode. In this mode the device is biased above breakdown voltage V_b by an amount ΔV . The voltage remains at this value until a breakdown is initiated following the generation, either thermally or optically, of a primary e-h pair, one carrier of which enters the multiplying region of the depletion layer to initiate the discharge. In silicon the ionization coefficient of an electron is much greater than that of a hole, and so the device is designed so that the carrier initiating the breakdown is normally an electron. Thus the expression photoelectron detection probability is only a slight misnomer and is meant to include those hole-initiated detected events.

Not all primary pairs succeed in initiating a discharge. Although conditions are such that, on the average, the number of carriers in the multiplying region increases exponentially with time, some just start a chain of ionizations that terminates, because of a fluctuation to zero carriers, before it really gets going, resulting in a relatively low gain ($1 \sim 10^4$). The probability that the chain of ionizations continues to increase until the whole diode is discharged is called the breakdown probability, P_b . It can be calculated,^{9,10} provided the electric-field profile and the e-h ionization coefficients are known. The calculated value of P_b is plotted as a function of ΔV in Fig. 2 for two different APD designs. It has a form that can be approximated, at least for small ΔV 's, by

$$P_b = 1 - \exp(-\Delta V/V_c),$$

where characteristic voltage V_c depends on the depletion layer thickness and on k_{eff} ,⁸ which is a weighted average of the ratio of the ionization coefficient of holes to that of electrons. This is a function of the

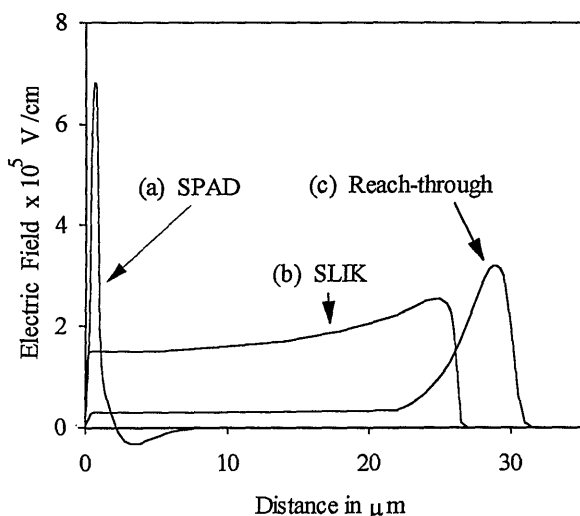


Fig. 1. Field profile of three APD structures that can be used for photon counting: (a) the SPAD (a single-photon APD) developed by Cova *et al.*, (b) reach-through structure; (c) Slik design.

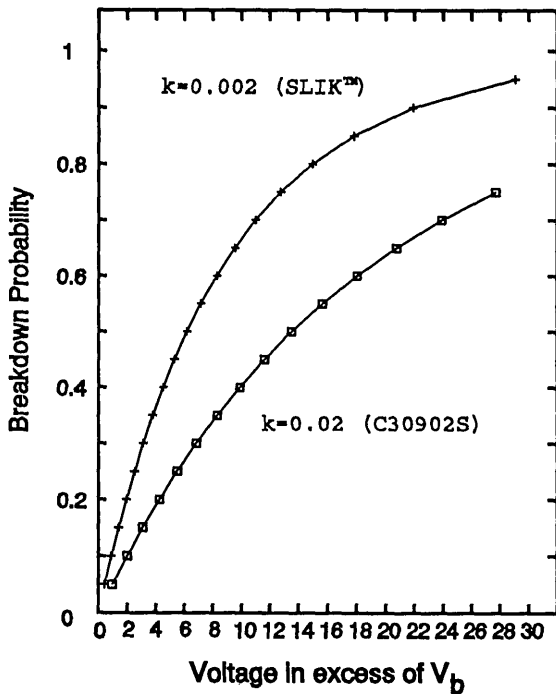


Fig. 2. Breakdown probability for two types of APD as a function of the applied voltage in excess of V_b (the voltage at the onset of breakdown).

device design. The data discussed in this paper pertain primarily to the two different diode structures: a standard structure (i.e., EG&G C30902S) for which $k_{\text{eff}} = 0.02$ and $V_c \sim 16$ V, and a Slik structure for which $k_{\text{eff}} = 0.002$ to 0.004 (depending on wavelength) and $V_c \sim 8$ – 9 V.

As stated above, not all primary pairs result in a breakdown. The fraction of $1 - P_b$ that does not break down can still result in gains ranging from unity (no ionizing collisions) to $\sim 10^4$. If a low-noise preamplifier is used and the comparator threshold is low enough to be triggered by some of these, then photoelectron detection probability P_e in the Geiger mode can be greater than breakdown probability P_b .

Experimentally, the measured value of P_b (i.e., P_e measured with a high threshold) is often less than the calculated value. The cause of this discrepancy is believed to be space-charge effects, which can result in some of the pulses self-quenching after only a small reduction in ΔV ; these pulses will be missed if the threshold is set too high.

Sub-Geiger-mode operation: In this mode, the APD is biased within a volt or two of its breakdown voltage (i.e., at a voltage at which the average gain is in the 500–2000 range), and the diode is used in conjunction with a low-noise charge-sensitive preamplifier with a noise-equivalent charge of a few hundred electrons and a comparator with a threshold set at 5–6 times the amplifier noise level. The APD is then capable of counting those pulses for which the gain happens to exceed the threshold level. In this mode P_e is dependent on k_{eff} and on the preamplifier noise level. The potential advantage of this mode is

that it avoids, to a great extent, factors such as diode heating, dead time, and afterpulsing, which limit the maximum achievable count rate in the Geiger mode (see below).

Figure 3 shows the calculated value of P_e , in both the Geiger ($V > V_b$) and sub-Geiger modes ($V < V_b$) for k_{eff} values of 0.02 and 0.002, as a function of the comparator threshold setting and parameter δ/δ_b (which is roughly proportional to V/V_b):

$$\delta = \int_0^w \alpha dx,$$

where α is the electron ionization coefficient, w is the thickness of the device, and δ_b is the value of δ at the breakdown voltage. The dashed curves in Fig. 3 show P_b , which is the value of P_e in the Geiger mode at high threshold settings. It is seen that although P_e is greater in the Geiger than in the sub-Geiger mode, respectable values of P_e can be achieved in the sub-Geiger mode, particularly with the lower k_{eff} device, provided the threshold level can be kept sufficiently low. This is normally possible for wideband preamplifiers, if the detector capacitance is small.

Practical Limitations to Geiger-Mode Operation

Some of the factors that limit the maximum count rate and the linearity of APD's used in the Geiger mode are diode heating, dead time, reignition, and afterpulsing.

Diode heating: Diode heating is a major limitation in the EG&G C30902S APD, which was designed initially for low-power operation in the linear mode. In the packaging of this device, the detector chip is mounted upon the end of a central contact pin; heat is conducted to the outside world primarily via this pin, resulting in a thermal resistance of ~ 1 °C/mW. The energy dissipated in the diode per pulse is roughly $\Delta VC_i V_b$, or $\sim 10^{-8}$ J or more per pulse, for a

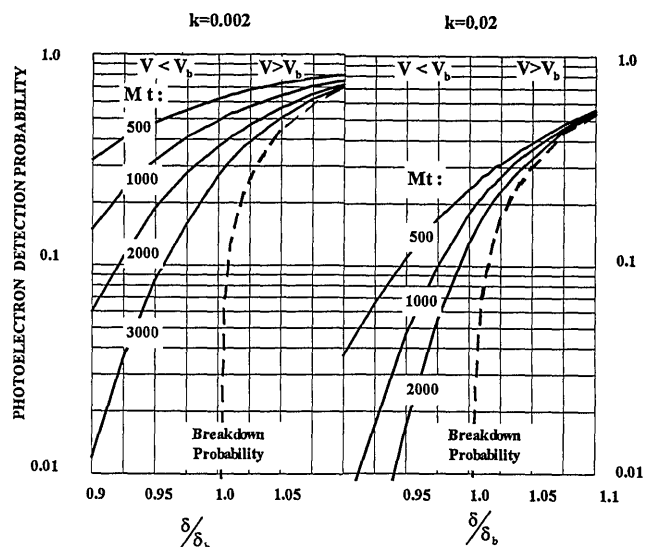


Fig. 3. Single-photon detection probability as a function of discriminator threshold setting Mt (in electrons) for two types of APD.

total dissipation of ~ 10 mW at a count rate of 10^6 /s. Since the temperature coefficient of the breakdown voltage is ~ 0.75 V/ $^{\circ}$ C, such an increase in temperature, and thus in V_b , would reduce ΔV significantly unless the applied voltage is also increased to compensate. Note that this is a problem of the heat sink and not of the diode itself; the same diode, mounted upon a temperature-regulated heat sink, will have a counting-rate reduction caused by diode heating that is ~ 2 orders of magnitude less.

This effect can best be seen by the use of light transients. Figure 4 shows the effect of a step variation in light intensity. Figure 4(a) shows the results obtained with an EG&G C30902S APD in its standard case, Fig. 4(b) shows the results obtained with the same device on a better heat sink, and Fig. 4(c) shows the results obtained with the Slik detector mounted upon a temperature-controlled thermoelectric cooler [standard single-photon-counting module (SPCM) assembly]. One can see that good temperature regulation is absolutely necessary if errors that are due to heating effects are to be kept to a minimum. The measured fluctuation in the counting rate, for a standard SPCM assembly, is 0.5% per Mc/s.

Dead time: In the Geiger mode the dead time depends primarily on the type of quench circuit used,

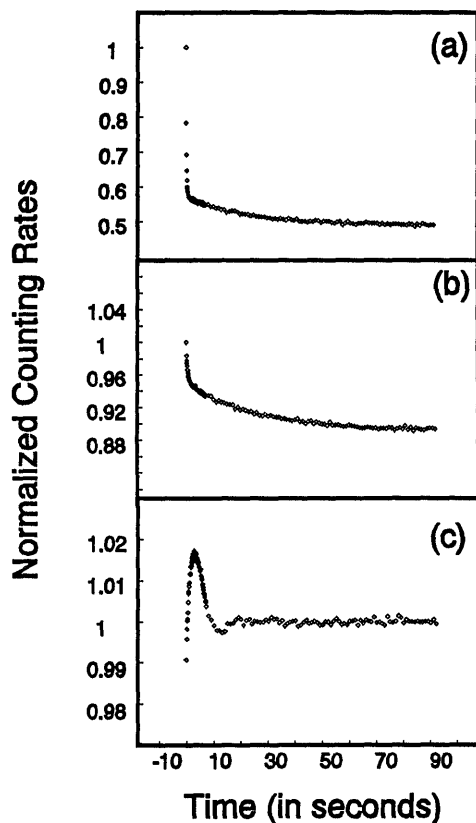


Fig. 4. Response of various APD assemblies to a step variation in light intensity (100 ns per data point): (a) Standard C30902S package (step variation in power dissipation in APD 3 mW); (b) C30902S chip mounted upon ceramic (step variation in power dissipation in APD 10 mW); (c) standard SPCM-100-PQ (step variation in power dissipation in APD 10 mW).

the two usual approaches being passive and active quenching.¹¹ For an excellent review of the use of APD's in these modes, particularly with respect to the requirements of photon correlation systems, see Brown *et al.*^{12,13}

In the passive quenching mode, a large series resistor is used to ensure that the steady-state current through the diode after breakdown is less than the latching current. Below this value the current tends to quench itself in a few nanoseconds, following which the diode recharges in a time determined by the RC product of this resistor and total C_t of the diode and stray capacitance. The latching current depends on the device uniformity; typical values are in the 40–100- μ A range. Since larger values of the series resistor will both permit higher ΔV 's and lengthen the recharge time, there is a trade-off, when purely passive quenching is used, between the photoelectron detection efficiency and the maximum counting rate. If a high counting rate or a short dead time is not a requirement, passive quenching represents a simple and perfectly satisfactory mode of operation. However, the relatively slow recharge time limits the maximum count rate.

If higher count rates or shorter dead times are required, an active quench circuit should be used. In this approach an attempt is made to sense the onset of the discharge as early as possible and, through external circuitry, reduce the diode voltage as quickly as possible to a value several volts below the breakdown voltage so as to ensure complete termination of the diode current in the multiplying region. The voltage can then be restored to its original value to await the next photon. A satisfactory fast quench circuit has been developed in this laboratory with dead times as short as 50 ns, thus permitting counting rates of up to 10 Mc/s at correction factors of less than 2.

Figure 5(a) shows the autocorrelation function of a

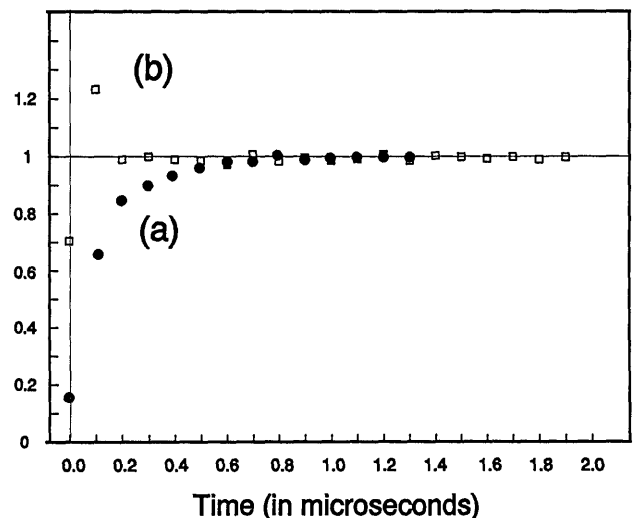


Fig. 5. Autocorrelation function, 100 ns per point. In both cases, the counting rate was approximately 30,000 cps: (a) SPCM-100-PQ, (b) C30902-S with the new active quenching circuit.

SPCM-100 with passive quenching (limiting resistor 200 K Ω) and an effective dead time of ~ 200 ns. Figure 5(b) shows an autocorrelation function for an actively quenched C30902S. Very little afterpulsing is indicated in either case. Also, the apparent dead time in the case of the active quench circuit was, in this measurement, limited by the correlator (with a minimum timing bin of 100 ns). Figures 6(a) and 6(b) show the measured values of the correction factors to be used to correct the measured counting rate to that which would be expected with zero dead time for the passively and the actively quenched SPCM's. Note that it almost exactly fits the theoretical curve, $[1 - (\tau_d Cr)]^{-1}$ (where Cr is the counting rate) for fixed dead times τ_d of 200 and 47 ns, respectively.

Reignition: This occurs when the quench circuit attempts to reset the voltage before the current from the previous pulse is completely terminated. This effect is particularly bothersome in diodes that are not particularly uniform in breakdown voltage. In these, the discharge current continues to trickle through the diode, limited by the local space-charge resistance, for times up to hundreds of nanoseconds after the initial discharge. This effect can be eliminated by ensuring that the quench circuit reduces the voltage on the diode to a few volts below the breakdown voltage for a few nanoseconds.

Afterpulsing has many of the characteristics of reignition and in the past has often been confused with it. True afterpulsing results from trapped carriers that are subsequently released later as a result of thermal excitation. Preliminary measurements in this laboratory indicate that the integral probability of a true afterpulse occurring more than 50 ns after the previous pulse is normally less than $\sim 0.5\%$, which is considerably less than originally reported,² with a primary detrapping time of ~ 100 ns or less unless the diode is cooled to below -20 $^{\circ}\text{C}$.

Factors Affecting Performance in the Sub-Geiger Mode

In theory, operation in the sub-Geiger mode has many advantages. Because the average gain is 4 to 5

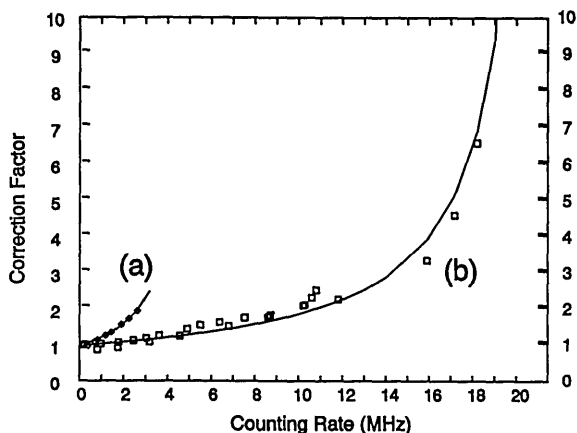


Fig. 6. Ratio of quantum efficiency times true photon rate/counting rate as a function of the counting rate for (a) an SPCM-100-passive quenching, (b) C30902S with the new active quench circuit.

orders of magnitude less than in the Geiger mode, factors such as diode heating, dead time, reignition and afterpulsing are no longer a problem. The diode itself responds in a time of the order of 1 ns. Thus the maximum counting rate is now determined by the bandwidth of the preamplifier or the recovery time of the comparator rather than that of the diode. Furthermore, since light emission will be greatly reduced, operation of integrated arrays of photon counting diodes with little optical cross talk would seem possible. In practice, achieving a high P_e in this mode has proven difficult. The detection of such small signals requires a very-low-noise preamplifier, with little or no pulse overshoot (to avoid apparent afterpulsing that is due to circuit transients). Good shielding is also important for avoiding radio frequency interferences since the signals being sensed are very small. Because P_e varies rapidly with ΔV (see Fig. 2) this approach requires a diode in which the breakdown voltage is uniform, within a volt or two, everywhere in the sensitive region. For the same reason, the circuit must maintain the temperature constant within a fraction of a degree if P_e is to remain constant. Thus, while operation at counting rates in excess of 50 Mc/s with dead times in the 10–20-ns range, seems possible, to our knowledge no sub-Geiger-mode circuit with a satisfactory detection efficiency has yet been built.

Recent Progress on Photon Counting Devices and Circuits

Diodes: A continuing problem with diodes such as the C30902S and the Slik structures, which have an etched well in the sensitive region to reduce the active thickness to the desired value of 30 μm , is the difficulty of achieving a uniform thickness in the well. A 1- μm variation in thickness will result in a breakdown voltage variation of 2–3 V in a C30902S and as much as 15 V in a Slik. Recently, techniques of handling very thin wafers have been developed, which permit these devices to be manufactured without wells. This has permitted diodes of the C30902S structure to be fabricated with diameters of as much as 1 mm and Sliks with diameters of as much as 0.5 mm with encouragingly uniform gains.

A new process has been developed that reduces the effective thickness of the surface dead layer, thereby increasing the quantum efficiency at short wavelengths. Figure 7 shows the quantum efficiency measured on a diode made by the use of the new process and antireflection coated at ~ 500 nm, compared with standard devices (which are antireflection coated at ~ 800 nm).

Passive quench circuits: Passive quenching is simple to implement, requires a minimum of power or space, and is robust. EG&G's SPCM-100/200-PQ modules⁵ (with integral thermoelectric cooling, temperature control, high-voltage supply, and transistor-transistor logic comparator) offer useful counting from 10 to 10^5 cps with photon detection efficiencies on standard units in the 20–50% range, depending on

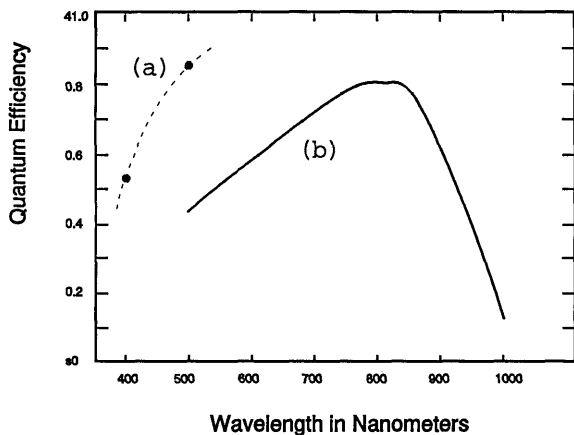


Fig. 7. Measured quantum efficiency: (a) New experimental process (antireflection coating at 500 nm), with no window in front of the detector; (b) standard C30902S (antireflection coating at 820 nm).

wavelength. Control of the thermoelectric cooler is fast enough so that even in a rapidly fluctuating light level the response is almost constant [see Fig. 4(c)].

Two recently reported results on passively quenched Geiger-mode APD's at high ΔV 's are of considerable interest.

(1) Using a parametric downconverter two-photon technique,¹⁴ which permits the photon detection probability to be measured absolutely, Kwiat *et al.*¹⁵ has reported detection efficiencies of 61.7% and 69.4% at 633 nm on two EG&G SPCM-200 modules that were modified to permit operation at an overvoltage (ΔV) of 30 V. These detection efficiencies are consistent with the expected quantum efficiency ($\sim 80\%$) and the theoretical photoelectron detection efficiency ($\sim 85\%$) at this overvoltage.

(2) Using a passively quenched 150- μm Slik detector mounted on a thermoelectric cooler in a module modified to permit matching to a 50- Ω output line, Li *et al.*¹⁶ have measured a timing jitter of 168 ps FWHM at 533 nm at an overvoltage of 20 V. This timing jitter is considerably less than what has been observed previously on C30902S's¹⁷ or with Slik detectors at lower overvoltages.

Active quench circuits: A number of active quench circuits have been described in the literature.^{12,18-20} In general, these circuits, if sufficiently fast, are capable of handling only relatively small values of the overvoltage. Cova *et al.* have reported¹⁸ an active quench circuit that switches up to 40 V above the breakdown. An active quench circuit (Fig. 8) has been developed at EG&G for which ΔV can be as high as 20 V and for which the dead time is ~ 50 ns. This time is determined primarily by the speed of the comparator and the electronics used to quench the avalanche. It is expected that the dead time can be reduced to ~ 25 ns or less.

An important feature of this circuit design is that the voltage is first reduced to a value of a few volts

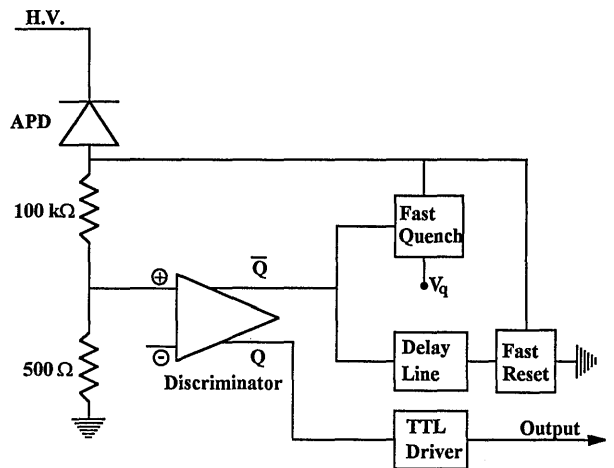


Fig. 8. Schematic diagram of the active quench-active reset circuit. V_q , quenching voltage (up to 25 V); TTL, transistor-transistor logic; H.V., high voltage.

below the breakdown voltage to ensure that the previous pulse has stopped completely before the applied voltage is reset. Another important feature is that the quench voltage is applied as early as possible so as to divert as much of the diode charge as possible away from the APD. This minimizes after-pulsing and light emission. Figure 9(a) shows the waveform of the quenching signal applied to the detector, and Fig. 9(b) shows the current that is due to the discharge, through the APD, of the parasitic capacitors. The avalanche starts to be quenched

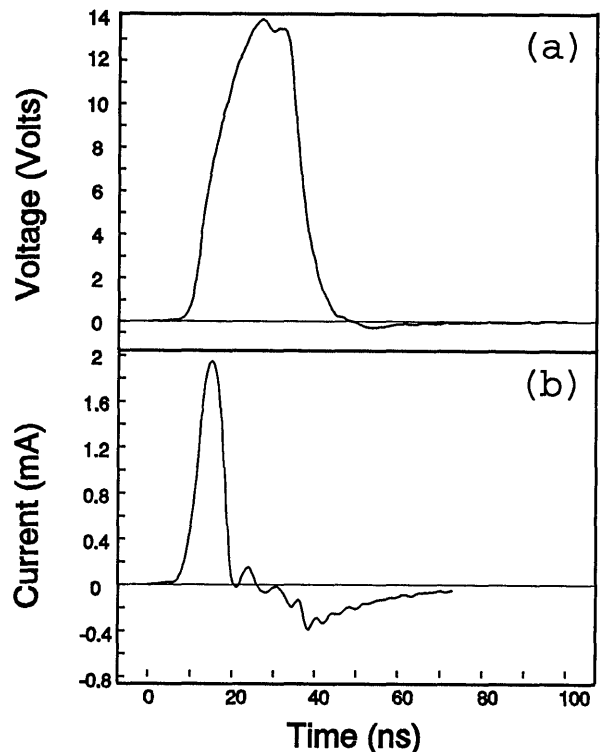


Fig. 9. Waveforms measured with a C30902S and the active quench circuit: (a) Variation of voltage across the APD, (b) current flowing through the diode.

very early and remains quenched well after the current has stopped. This is the same circuit as was discussed above [Figs. 5(b) and 6(b)].

Sub-Geiger-mode operation: Sun and Davidson²¹ have reported operation in the sub-Geiger mode with a C30902S and a 700-MHz preamplifier, followed by a 200-MHz filter. They achieved a photon detection efficiency of 5% at 820 nm and a dead time of 15 ns, which was limited primarily by the speed of the comparator used. As they pointed out, they would have expected better results with a narrower bandwidth (lower noise) preamplifier.

Using a hybrid preamplifier with a bandwidth of 60 MHz, we have achieved a detection efficiency of ~10% within our own laboratory. This, too, was less than expected and, we believe, was limited by noise pickup. Efforts to improve this setup will continue.

Summary

New APD's with improved quantum efficiencies and gain uniformities that are suitable for photon counting in photon correlation and other systems have been described. Techniques of using these devices to attain high photon detection efficiencies (approaching 70%), excellent timing characteristics (sub-nanosecond timing jitter) and small dead times (~50 ns) have been described. These devices and techniques are still in the research stage; it is planned to have them commercially available eventually.

References and Notes

1. R. J. McIntyre, "Recent developments in silicon avalanche photodiodes," *Measurement* **3**, 146-162 (1985).
2. A. W. Lightstone and R. J. McIntyre, "Photon counting silicon avalanche photodiodes for photon correlation spectroscopy," in *Photon Correlation Techniques and Applications*, Vol. 1 of OSA Proceedings Series (Optical Society of America, Washington, D.C., 1988, pp. 183-191).
3. A. W. Lightstone, A. D. MacGregor, D. E. MacSween, R. J. McIntyre, C. Trottier, and P. P. Webb, "Photon counting modules using RCA silicon avalanche photodiodes," preprint from CP-100933, NASA Laser Light Scattering Advanced Technology Workshop—1988 (NASA Lewis Research Center, Cleveland, Ohio, 1988).
4. EG&G C30902S/C30921S data sheet (EG&G Canada Ltd., Vaudreuil, Quebec, Canada).
5. EG&G SPCM-100/200-PQ data sheet (EG&G Canada Ltd., Vaudreuil, Quebec, Canada).
6. See, for example, S. Cova, G. Ripamonti, and A. Lacaita, "Avalanche semiconductor detector for single optical photons with a time resolution of 60 ps," *Nucl. Instrum. Methods* **A253**, 482-487 (1987).
7. S. Cova, Dipartimenti di Elettronica, Politecnico di Milano, 20133 Milan, Italy (personal communication, 1992).
8. See, for example, P. P. Webb, R. J. McIntyre, and J. Conradi, "Properties of avalanche photodiodes," *RCA Rev.* **35**, 235-278 (1974).
9. W. G. Oldham, R. R. Samuelson, and P. Antognetti, "Triggering phenomena in avalanche diodes," *IEEE Trans. Electron Devices* **ED-19**, 1056-1060 (1972).
10. R. J. McIntyre, "On the avalanche initiation probability of avalanche-diodes above the breakdown voltage," *IEEE Trans. Electron Devices* **ED-20**, 637-641 (1973).
11. S. Cova, A. Longoni and A. Andreoni, "Towards picosecond resolution with single-photon avalanche diodes," *Rev. Sci. Instrum.* **52**, 408-412 (1981).
12. R. G. W. Brown, K. D. Ridley, and J. C. Rarity, "Characterization of silicon avalanche photodiodes for photon correlation measurements. 1: Passive quenching," *Appl. Opt.* **25**, 4122-4126 (1986).
13. R. G. W. Brown, K. D. Ridley, and J. C. Rarity, "Characterization of silicon avalanche photodiodes for photon correlation measurements. 2: Active quenching," *Appl. Opt.* **26**, 2383-2389 (1987).
14. J. G. Rarity, K. D. Ridley, and P. R. Tapster, "An absolute measurement of detector quantum efficiency using parametric downconversion," *Appl. Opt.* **26**, 4616-4619 (1987).
15. P. Kwiat, A. Steinberg, M. Petroff, P. B. Eberhard, and R. Chiao, University of California, Berkeley, Berkeley, California 94720 (personal communication).
16. L.-Q. Li, L. M. Davis, S. I. Soltesz, and C. J. Trottier, "Single photon avalanche diode for single molecule detection," in *Annual Meeting*, Vol. 23 of 1992 OSA Technical Digest Series (Optical Society of America, Washington, D.C., 1992), p. 137.
17. M. Ghioni and G. Ripamonti, "Improving the performance of commercially available Geiger-mode avalanche photodiodes," *Rev. Sci. Instrum.* **62**, 1-5 (1991).
18. S. Cova, A. Longini, and G. Ripamonti, "Active quenching and gating circuits for single photon avalanche photodiodes (SPADs)," *IEEE Trans. Nucl. Sci.* **NS-29**, 599-601 (1982).
19. N. S. Nightingale, "A new silicon avalanche photodiode photon counting detector for astronomy," *Exp. Astron.* **1**, 407-422 (1991).
20. T. O. Regan, H. C. Fenker, J. Thomas, and J. Oliver, "A method to quench and recharge avalanche photodiodes for use in high-rate situations," *Nucl. Instrum. Methods* (to be published).
21. X. Sun and F. M. Davidson, "Photon counting with silicon avalanche photodiodes," *J. Lightwave Technol.* **10**, 1023-1032 (1992).